MOLECULAR AND CELLULAR BIOLOGY, Feb. 1986, p. 365–371
0270-7306/86/020365-07$02.00/0
Copyright © 1986, American Society for Microbiology
Vol. 6, No. 2

Murine Dihydrofolate Reductase Transcripts through the Cell Cycle

PEGGY J. FARNHAM AND ROBERT T. SCHIMKE*
Department of Biological Sciences, Stanford University, Stanford, California 94305

Received 5 August 1985/Accepted 23 October 1985

The murine dihydrofolate reductase gene codes for mRNAs that differ in the length of their 3′ untranslated region as well as in the length of their 5′ leader sequence. In addition, the dihydrofolate reductase promoter functions bidirectionally, producing a series of RNAs from the opposite strand than the dihydrofolate reductase mRNAs. We have examined the production of these RNAs and their heterogeneous 5′ and 3′ termini as mouse 3T6 cells progress through a physiologically continous cell cycle. We found that all of the transcripts traverse the cell cycle in a similar manner, increasing at the G1/S boundary without significantly changing their ratios relative to one another. We conclude that cell-cycle regulation of dihydrofolate reductase is achieved without recruiting new transcription initiation sites and without a change in polyadenylation sites. It appears that the mechanism responsible for the transcriptional cell-cycle regulation of the dihydrofolate reductase gene is manifested only by transiently increasing the efficiency of transcription at the dihydrofolate reductase promoter.

The mouse dihydrofolate reductase (DHFR) gene spans approximately 31 kilobase pairs of DNA from the initiation codon to the end of the sequences coding for the largest major mRNA (5). The six exons constituting the coding region consist of 558 base pairs, with the remaining 30 kilobase pairs divided into five intervening sequences (see Fig. 1A). There are four major and two minor RNA transcripts which differ in the length of their 3′ untranslated region (18; C. S. Gasser and R. T. Schimke, submitted for publication). In addition, there are two sites of transcription initiation (S. Sazer and R. T. Schimke, submitted for publication) and minor sites further upstream (4, 9, 16). No functional differences among the various DHFR 5′ or 3′ termini have been discerned, nor have their ratios been found to change consistently under any conditions.

The DHFR promoter functions bidirectionally to produce RNAs oriented in the direction opposite to the DHFR mRNAs (8). These opposite-strand RNAs also have heterogeneous starts, comprising six sites ranging over a 60-base-pair region. These RNAs are complementary to 180 to 240 nucleotides of the 5′-flanking region of the DHFR gene. Although these RNAs are most abundant in nuclear, nonpolyadenylated RNA (8), their presence as part of a longer transcript cannot be totally ruled out (4). Although the function of the opposite-strand RNAs is unknown, it is possible that they are involved in the regulation of the DHFR gene. Determining whether they fluctuate differently or whether they exhibit the same cell cycle increase as DHFR mRNA might provide insight into the mechanism by which the DHFR gene is cell-cycle regulated.

We have shown previously that the DHFR gene is cell-cycle regulated at the transcriptional level (9). However, the utilization of the different 5′ and 3′ termini has not been examined throughout the cell cycle. It is possible that different initiation or polyadenylation signals, or both, are used in the burst of transcription in S phase than are used during the constitutive expression of the gene. To answer this question, we have examined DHFR transcripts as cells progressed through a single, physiologically continuous cell cycle.

* Corresponding author.

MATERIALS AND METHODS

DNA constructions. The plasmid pSP65-RT10$^+$ contains a 1,017-base-pair *Eco*RI/*Hin*dIII fragment derived from the 5′ end of the mouse DHFR gene and inserted into the *Eco*RI and *Hin*dIII sites of plasmid pSP65 (Promega Biotec) as previously described (8). The plasmid pSP64-RT10$^-$ contains the identical fragment inserted in the opposite orientation into the plasmid pSP64 (Promega Biotec). The plasmid pMg0 (10) contains 1.0 kilobase of DHFR 5′-flanking sequence, the complete coding region of the DHFR gene (without introns), and a portion of the 3′ noncoding sequences cloned into pBR322. The plasmid pSP64-3′ was created by isolation in Sea Plaque agarose of the approximately 1,200-base-pair *Pst*I/*Sst*I fragment derived from the DHFR cDNA clone pDHFR11 (17) and subsequent ligation into the *Pst*I and *Sst*I sites of pSP64 according to the method of Crouse et al. (3). The insert corresponds to the last 307 nucleotides of DHFR coding sequence and 880 nucleotides of the 3′ noncoding region. The plasmid pSP65-3′ contains the same *Pst*I/*Sst*I fragment inserted in the opposite orientation in pSP65. The ligation products were transformed into *Escherichia coli* HB101 (6), and plasmid DNA was obtained by standard procedures (7).

Cell lines. The mouse cell lines used in these studies included 3T6 cells (2) and the methotrexate-resistant cell line 3T6 R50-MS6-clone A, which contains 50 copies of the DHFR gene (9). The cell line 200–1 was constructed by transfection of genomic DNA from the methotrexate-resistant mouse cell line L5178Y CR200 into DHFR-dificient Chinese hamster ovary cells (see Gasser and Schimke [submitted] for details). The resultant cell line, 200–1, contains at least 3.7 kilobase pairs of 5′-flanking sequence and 6.5 kilobase pairs of 3′ flanking sequence, produces DHFR transcripts and protein that are indistinguishable from those of mouse cells, and yet does not cell-cycle regulate DHFR.

Isolation and quantification of cell cycle RNA. An important consideration in studying cell-cycle regulation is the method used to obtain stage-specific RNAs. Synchronization techniques such as serum or amino acid starvation or growth to confluency severely alter the normal cell cycle, resulting in a G0-like state from which the cells must emerge before

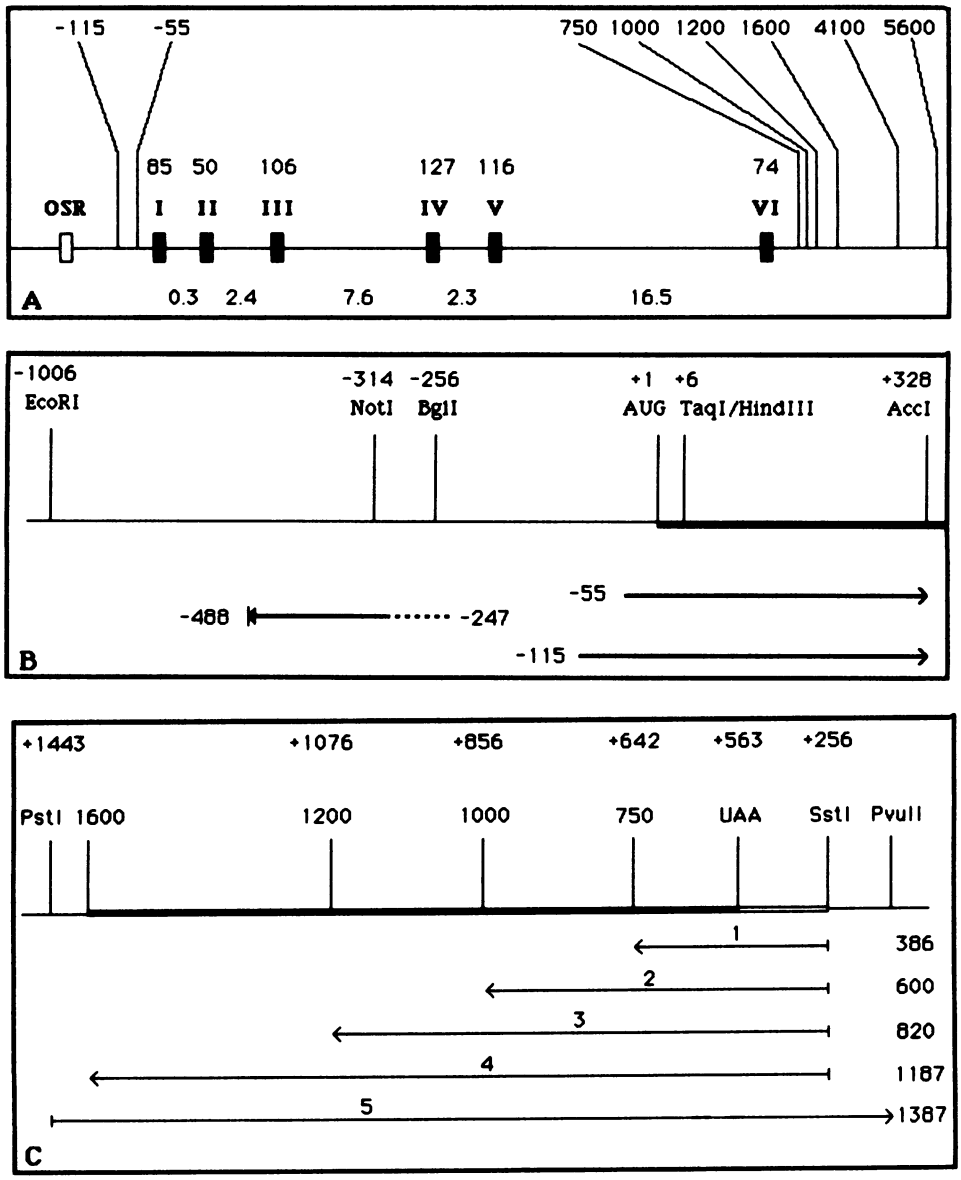

FIG. 1. (A) Genomic organization of the DHFR gene. The six exons are represented by black boxes with sizes in base pairs above each exon. The sizes of the five introns are in kilobase pairs. The six DHFR polyadenylation sites are indicated after exon 6. The two transcription initiation sites are indicated in the 5′ region. The open box represents the region of the 5′-flanking sequences complementary to the opposite-strand RNAs (OSR).(B) The 5′ end of the DHFR gene as represented in Mg0. The heavy line represents coding sequences (derived from a cDNA clone). The two major start sites of DHFR mRNAs are shown by the open arrows; the heterogeneous starts of the opposite-strand RNAs are represented by the dashed lines in the closed arrowhead. Restriction sites are numbered at the cutting site. (C) The 3′ end of the DHFR gene. Coding sequences (open line) and 3′ noncoding sequences (solid thick line) and their relationship to vector (thin line) restriction sites are shown. Only restriction sites derived from the murine DNA are numbered (+1 is the A of the translation start codon). The size of the protected fragments for each of the four DHFR mRNAs is indicated, along with the complete probe (5). Transcription of the RNA probe begins approximately 15 nucleotides 5′ of the *PstI* site and continues 185 nucleotides beyond the *SstI* site to the vector *PvuII* site.

entering the normal G1-to-S progression. That these perturbations can influence the regulation of a particular gene is demonstrated in the case of the c-*myc* oncogene. Although cell-cycle regulation of c-*myc* mRNA levels was demonstrated, using serum deprivation to synchronize cells, the opposite results were obtained by density arrest (19) or centrifugal elutriation (11). In addition, previous studies of the DHFR gene have produced contrasting results when serum starvation versus density arrest was used (see reference 9 for details). Because of this, we chose a selection, rather than an induction, method of synchronization which allowed us to examine DHFR mRNA throughout an unperturbed cell cycle.

To obtain mRNA from specific times in the cell cycle, 3T6 R50 cells were synchronized by mitotic selection from 175-cm^2 flasks (for details, see reference 9). The cells were harvested at 2, 6, 8, 10, 12, or 16 h after mitotic selection, and total RNA was isolated. The cells (0.5×10^6 to 1.5×10^6 cells per 100-cm^2 dish) were rinsed twice with cold Hanks balanced salt solution and lysed in 1 ml of a 1:1 solution of lysis buffer (0.14 M NaCl, 1.5 mM $MgCl_2$, 10 mM Tris chloride [pH 8.6], 0.5% Nonidet P40, and 10 mM vanadyl

ribonucleoside complexes) and 2× PK buffer (0.2 M Tris chloride [pH 7.5], 25 mM EDTA 0.3 M NaCl, 2% [wt/vol] sodium dodecyl sulfate) containing 24 μg of protein-free tRNA (*E. coli*) and 200 μg of proteinase K. Approximately 30,000 cpm of in vivo [^{3}H]uridine-labeled RNA from parental 3T6 cells was included in the lysis mixture to monitor the RNA isolation. After a 30-min incubation at 37°C, the solution was extracted with 1 ml of phenol-chloroform-isoamyl alcohol (24:24:1) and then precipitated with 2.5 volumes of ethanol for at least 2 h at −20°C. The mixture was centrifuged at 8,000 rpm for 20 min at 0°C in an HB4 rotor, washed with 70% ethanol–0.1 M sodium acetate (pH 5.2), and recentrifuged at 8,000 rpm for 10 min. The nucleic acids were dissolved in 200 μl of 50 mM Tris (pH 7.4)–1 mM EDTA–10 mM $MgCl_2$–2 mM vanadyl ribonucleoside complexes and 3 μg of RNase-free DNase per ml and incubated at 37°C for 30 min. At this point, EDTA and sodium dodecyl sulfate were added to 10 mM and 0.2% final concentrations, respectively, and the solution was extracted with an equal volume of phenol-chloroform-isoamyl alcohol. The RNA was precipitated with 0.5 volume of 7.5 M ammonium acetate and 3 volumes of ethanol and resuspended in water. At the final stage of preparation, a sample of RNA was counted to ensure that the isolation procedure was quantitative. When the increase in steady-state levels of DHFR RNA at the G1/S boundary was demonstrated (Fig. 2b, lanes 1 through 4; 3a, lanes 1 through 4; and 4a, lanes 1 through 4), RNA from an equal number of cells in each hour of the cell cycle was used in the protection experiments. A comparison based on the amount of DHFR RNA per cell is essential since the amount of rRNA increases dramatically during the cell cycle. A comparison based only on RNA mass (which is predominatly rRNA) could mask the cell-cycle regulation of a specific mRNA.

RNA protection experiments. Cell line 3T6 R50 cell-cycle whole-cell RNA was prepared as described above, and cytoplasmic RNA was prepared by the method of Maniatis et al. (14). Cytoplasmic and nuclear RNAs from the cell line 200–1 were provided by J. Feder.

To analyze the 5′ and 3′ ends of the DHFR mRNAs and the opposite-strand RNAs, the SP6 promoter system (Promega Biotec) was used. When linearized at the *Eco*RI site, pSP64-RT10$^-$ produced runoff transcripts complementary to the entire *Hin*dIII-to-*Eco*RI fragment and thus could be used to examine the 5′ ends of the DHFR mRNAs (see Fig. 1B). Conversely, linearizing pSP65-RT10$^+$ at the *Hin*dIII site produced runoff transcripts complementary to RNAs coded from the opposite strand to DHFR and thus could be used to examine the 5′ ends of the opposite-strand RNAs. In addition, the plasmid pSP65-RT10$^+$ was linearized at the *Not*I site to produce a runoff probe complementary to most of the length of the opposite-strand RNAs, ending just 3′ of the heterogeneous start sites (see Fig. 1B), and thus displayed the opposite-strand RNAs as a single band. The pSP64–3′ plasmid was linearized at the *Pvu*II site to produce a 1,387-base-pair runoff RNA probe complementary to the four major DHFR 3′ ends. pSP65–3′ was also linearized at the *Pvu*II site to produce a 1,387-base-pair probe with the same orientation as the DHFR mRNAS which would detect any RNAs transcribed from the opposite strand of the 3′ noncoding region. Approximately 2×10^6 to 4×10^6 cpm of RNA probe and 2 to 10 μg of cellular RNA were used in each RNA protection experiment, performed as described by Farnham et al. (8).

A 584-base-pair *Bgl*I/*Acc*I fragment and a 1,334-base-pair *Eco*RI/*Acc*I fragment spanning the DHFR promoter region were used as DNA probes in S1 nuclease reactions to examine the 5′ ends of the DHFR mRNAs. The plasmid pMg0 (10) was digested with *Acc*I, 5′ end-labeled with [γ-^{32}P]ATP using polynucleotide kinase (Bethesda Research Laboratories, Gaithersburg, Md.), digested with *Bgl*I or *Eco*RI, and separated by agarose gel electrophoresis. The promoter-containing fragments were isolated from the gel and purified on an Elutip-d column (Schleicher & Schuell, Inc., Keene, N.H.). Approximately 50,000 cpm of DNA probe and 1 to 5 μg of cellular RNA were used in each reaction, performed as described by Farnham and Schimke (9).

RESULTS

Cell-cycle analysis of the heterogeneous 5′ ends of DHFR mRNAS. Previous studies (9) had examined promoter utilization at 2 and 8 h into the cell cycle, using S1 RNA protection experiments. However, it has recently been shown that although under those S1 conditions the −115 start site (relative to AUG codon) is detected, the major DHFR start site at −55 is not. This is due to differences in the length and relative GC content of the 5′ noncoding regions of these two transcripts, resulting in their differential ability to form stable hybrids with that particular DHFR DNA probe. Detailed analysis confirming that position −55 represents an authentic transcription start site is presented elsewhere (Sazer and Schimke, submitted). We have now extended the cell-cycle analysis and used alternative RNA protection procedures to examine the heterogeneous 5′ ends of the DHFR mRNAs. Using a uniformly labeled *Hin*dIII/*Eco*RI RNA probe in protection experiments, the two DHFR start sites are seen as a single band at −115 and a trimer at ≈55 in cytoplasmic RNA from unsynchronized 3T6 R50 cells (Fig. 2a, lanes 1 and 2). To determine whether the ratio of these start sites changes or whether a different start site is utilized at different times in the cell cycle, the cells were synchronized by mitotic selection, and RNA was isolated at 2, 6, 8, 10, 12, and 16 h into the cell cycle. By 16 h the cells have progressed from G1 through S and into G2 phase of the cell cycle (9). Figure 2b shows that there was no difference in the RNA protection pattern from 2 to 16 h. Lanes 1 through 4 show the start sites in 2-, 6-, 8-, and 10-h RNA from one mitotic selection. The analysis was extended to 6-, 8-, 12-, and 16-h RNA (lanes 5 through 8) from a second mitotic selection.

These experiments were repeated with end-labeled *Bgl*I/*Acc*I DNA probe in S1 reactions (Fig. 2c). Under these conditions, the −55 start appeared as a single band. The trimer seen with the RNA probe may be due to peculiarities of the RNase A or RNase T_1 digestion conditions. Figure 2c (lanes 6 through 11) shows that the start sites did not vary from 2 to 16 h in the cell cycle. The most likely point at which a difference would occur is at the burst of transcription at the G1/S boundary (9). Additional sets of mitotically selected RNA preparations (Fig. 2c, lanes 1 through 5) showed that the same start sites were used at 2 and 8 h. Although slight variations in the ratios of the two bands can be seen in lanes 1, 7, and 10, they were not reproducible (data not shown) and were not seen when the RNA probes were used. The 1,334-base-pair *Eco*RI/*Acc*I end-labeled probe was also used with 2 and 8 h RNA to determine whether any upstream starts were present which were not identified using the RNA probe. No additional bands were seen (data not shown).

Cell-cycle analysis of the heterogeneous 3′ ends of DHFR mRNAs. We next examined the 3′ ends of the four major

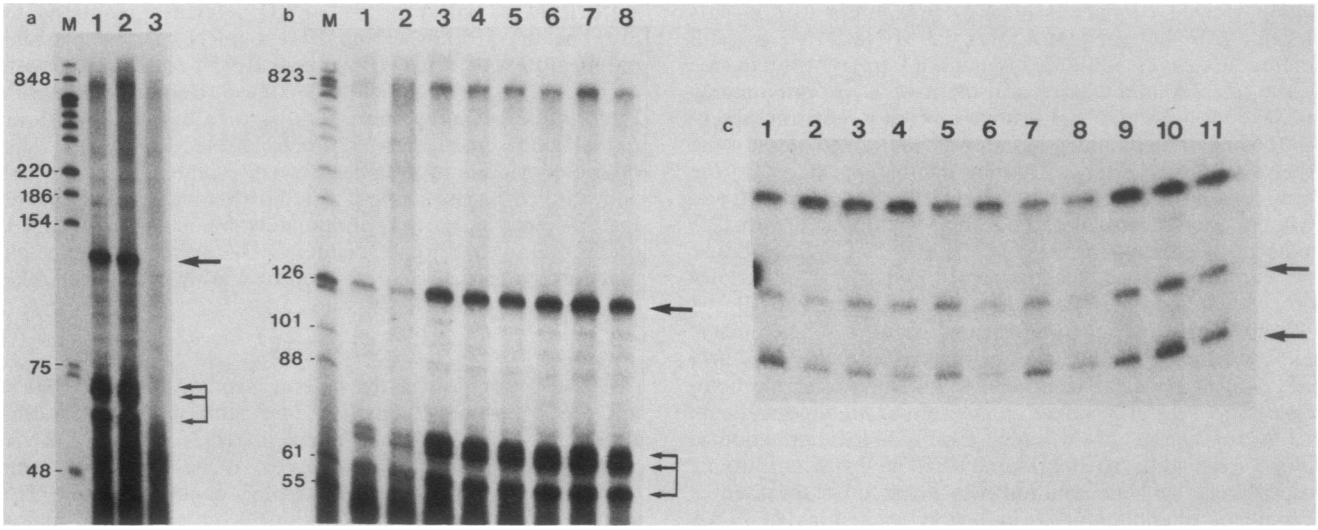

FIG. 2. (a) The 1,017-nucleotide, uniformly labeled *Hin*dIII/*Eco*RI RNA probe was used to identify the transcription initiation sites in 3T6 R50 total RNA preparations (lanes 1 and 2). The hybridization reaction in lane 2 contained twice as much probe to ensure the reaction was in probe excess. Lane 3 is a control using 3T6 parental RNA to show which bands were specific for DHFR. (b) The 1,017-nucleotide *Hin*dIII/*Eco*RI RNA probe was again used to examine the 5′ ends of the DHFR mRNAs in two separate mitotic selection experiments. Lanes 1 through 4 are from one synchronous population of 3T6 R50 cells and represent RNA from 2, 6, 8, and 10 h, respectively. RNA from an equal number of cells in each hour of the cell cycle was used in lanes 1 through 4 to demonstrate the increase in steady-state levels at the G1/S boundary and for a comparison with Fig. 3a (lanes 1 through 4) and 4a (lanes 1 through 4). The analysis was extended in a second mitotic selection experiment to include RNA from 6, 8, 12, and 16 h (lanes 5 through 8, respectively). (c) The 589-base-pair *Bgl*I/*Acc*I end-labeled DNA probe was used to examine the 5′ ends of DHFR mRNAs. RNA from 2, 6, 8, 10, 12, and 16 h (lanes 6 through 11, respectively) from 3T6 R50 synchronous cells was used. Also, additional separate preparations of 2-h RNA (lanes 1 and 2) and 8-h RNA (lanes 3 to 5) were included in the analysis. The upper arrow corresponds to RNA initiated at −115; the lower arrow corresponds to RNA initiated at −55. The unlabeled band is renatured probe.

DHFR mRNAs which have previously been identified by Northern analysis to be approximately 750, 1,000, 1,200, and 1,600 nucleotides in length (17). In addition, the 750- and 1,600-nucleotide mRNA 3′ ends have been mapped by sequencing cDNA clones (17), whereas the 1,000- and 1,200-nucleotide mRNAs were mapped to within 50 base pairs using S1 analysis (18). To map these four 3′ ends, we used a uniformly labeled RNA probe produced by the SP6 system. The ~1,200-base-pair *Sst*I/*Pst*I fragment from pDHFR11 was inserted into the SP6 promoter system in both orientations. Using the pSP65 clone, it was shown that no RNA is transcribed from the strand opposite to DHFR mRNA in this 1,200-base-pair 3′ noncoding region (data now shown). The pSP64 clone, however, detected the four major RNAs and two minor bands in both total and cytoplasmic 3T6 R50 RNA (Fig. 3a, lanes 5 and 6). A much longer exposure could also detect these same bands in RNA from 3T6 parental cells (not shown). The resolution of the gel allowed us to more precisely map the 3′ ends of DHFR mRNAs (see Fig. 1C). The 750- and 1,600-nucleotide mRNA 3′ ends correspond to those obtained by sequencing cDNAs from mouse S180 M500 cells. The 1,000- and 1,200-nucleotide RNAs have precise endpoints within the broad region defined by S1 mapping.

The ratio of the 750- and 1,600-nucleotide mRNAs by Northern analysis had not been consistent, ranging from equal amounts of the two RNAs to almost all of the 1,600-nucleotide mRNA (for examples, see reference 17). These quantitation problems might be explained by differential hybridization conditions of the two RNA/probe complexes. The Northern gels were probed with a cDNA of the 1,600-nucleotide mRNA, resulting in an RNA/probe homology twice as long for the 1,600-nucleotide mRNA than for the 750-nucleotide mRNA. The longer homology may be more stable during washing of the filter. This inconsistency precluded not only an estimate of the ratios of the RNAs in asynchronous populations, but also any examination of the change in 3′-end formation during the cell cycle. However, analysis by RNA protection experiments has been found to be very consistent; comparison of the two major 3′ ends repeatedly demonstrates an almost equal intensity of protected bands. In fact, an RNA sample which showed almost entirely 1,600-nucleotide mRNA when probed with a cDNA clone in Northern analysis (J. Feder, personal communication) showed the expected equal intensity of bands 1 and 4 in an RNA protection experiment (Fig. 3b, lane 6). Since the protected fragment corresponding to the 1,600-nucleotide mRNA is about three times as long as that corresponding to the 750-nucleotide mRNA (see Fig. 1C) and because the probe is uniformly labeled, it appears that there is at least threefold more of the 750-nucleotide mRNA than of the 1,600-nucleotide mRNA. Since the two very minor larger DHFR mRNAs (18; Gasser and Schimke, submitted) would also be represented in band 4 (see legend for Fig. 3a), this is a very slight overestimate of the amount of the 1,600-nucleotide mRNA.

We could now examine the pattern of the 3′ ends throughout the cell cycle, using the same stage-specific RNA as for the 5′ ends. No difference in the relative levels of the various 3′ ends occurred through 2, 6, 8, 10, 12, or 16 h in the cell cycle (Fig. 3a and b), implying that cell-cycle regulation is neither a cause nor a consequence of the heterogeneous 3′ ends.

Cell-cycle analysis of the heterogeneous 5′ ends of the opposite-strand RNAs. The DHFR promoter functions bidirectionally, and transcription initiation in the opposite

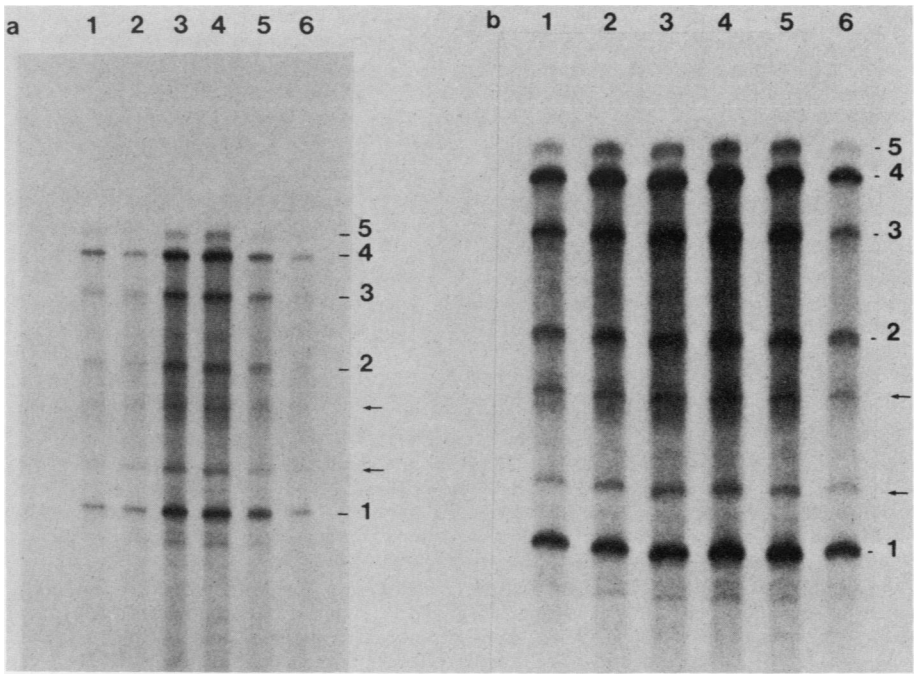

FIG. 3. Analysis of the 3′ ends of the DHFR mRNAs. (a) The 1,387-nucleotide uniformly labeled *Pst*I/*Pvu*II RNA probe was used to examine the 3′ ends of the DHFR mRNAs in 2-, 6-, 8-, and 10-h RNA (lanes 1 through 4 respectively) as well as in 3T6 R50 total RNA (lane 5) and cytoplasmic RNA (lane 6). RNA from an equal number of cells in each hour of the cell cycle was used in lanes 1 through 4 to demonstrate the increase in steady-state levels at the G1/S boundary and for a comparison with Fig. 2b (lanes 1 through 4) and 4a (lanes 1 through 4). The sizes of the bands were determined by comparison with known DNA markers (not shown due to different exposure time of the gel). The numbered bands represent the 3′ ends corresponding to (1) the 750-, (2) the 1,000-, (3) the 1,200-, and (4) the 1,600-nucleotide DHFR mRNA. There are two very minor DHFR mRNAs of 4,100 and 5,600 base pairs (18) which would also be represented in band 4 since their homology to the probe ends at +1443 (see Fig. 1C). The undigested probe is band 5. The arrows indicate the two minor bands discussed in the text. (b) The *Pst*I/*Pvu*II probe was again used in a second analysis of synchronized 3T6 R50 cells to show the 3′ ends in 6-, 8-, 10-, 12-, and 16-hr RNA (lanes 1 through 5, respectively). Lane 6 represents cytoplasmic 3T6 R50 RNA from asynchronously growing cells.

direction is also heterogeneous, consisting of a ladder of six starts approximately 10 base pairs apart (8). To examine the levels of the opposite-strand transcripts throughout the cell cycle, a uniformly labeled RNA probe extending from the *Eco*RI site to the *Not*I site was used (see Fig. 1B). This probe is complementary to almost the entire length of the RNAs but ends just 3′ to the last start site. This allows the ladder of bands to be visualized as one band. There was a dramatic increase in the levels of the opposite-strand RNA as the cells moved into S phase of the cell cycle (Fig. 4a). This increase parallelled that of the DHFR mRNAs seen in Fig. 2b, lanes 1 through 4, and Fig. 3a, lanes 1 through 4. The cell-cycle RNAs were also hybridized with the *Eco*RI/*Hin*dIII probe, which allows all six start sites to be visualized. As found with the DHFR mRNAs, the specificity of the opposite-strand start sites did not change significantly throughout the cell cycle (Fig. 4b).

The fact that the opposite-strand RNAs fluctuate through the cell cycle in the same manner as DHFR mRNAs implies that they are being regulated by the same mechanism as DHFR and are not themselves regulating DHFR. Another means of testing this is to examine their synthesis in cell lines in which DHFR is not cell-cycle regulated. One such cell line was produced by transfecting the mouse DHFR gene into DHFR-deficient hamster cells (Gasser and Schimke, submitted). This cell line, designated 200–1, contains the entire DHFR gene and extensive 5′- and 3′-flanking sequences and yet has lost the capacity for cell-cycle regulation during the transfection process. It is possible that a point mutation or small deletion occurred in a region critical for cell-cycle regulation during the transfection process. Although it has been shown previously (Gasser and Schimke, submitted) that the production of DHFR transcripts is not altered, it is possible that synthesis of the opposite-strand RNAs has been altered and is thus responsible for the loss of cell-cycle regulation. RNA from this cell line was examined for the presence of the opposite-strand RNAs by using the uniformly labeled *Eco*RI/*Not*I RNA probe. We found that, as in the normal mouse cells, the opposite-strand RNAs were being produced in about the same amounts as the DHFR mRNAs and were nuclear in location (Fig. 4c). This implies that the disruption of cell-cycle regulation in this cell line is not due to disorder in the opposite-strand RNA production.

DISCUSSION

Although the transcription pattern produced from the DHFR gene is quite complex, with heterogeneous starts from both directions of a bidirectional promoter and heterogeneous 3′ ends, we have shown that all of the transcripts traverse the cell cycle in a similar manner. That is, they all increase at the G1/S boundary without significantly changing their ratios relative to one another. We conclude that cell-cycle regulation is achieved without recruiting a new promoter and without a change 3′-end production of the DHFR mRNAs. Gasser and Schimke (submitted) have also shown that the normal 3′-end formation is not required for cell-cycle regulation of transfected DHFR minigenes. However, these studies did not examine the usage of the aberrant

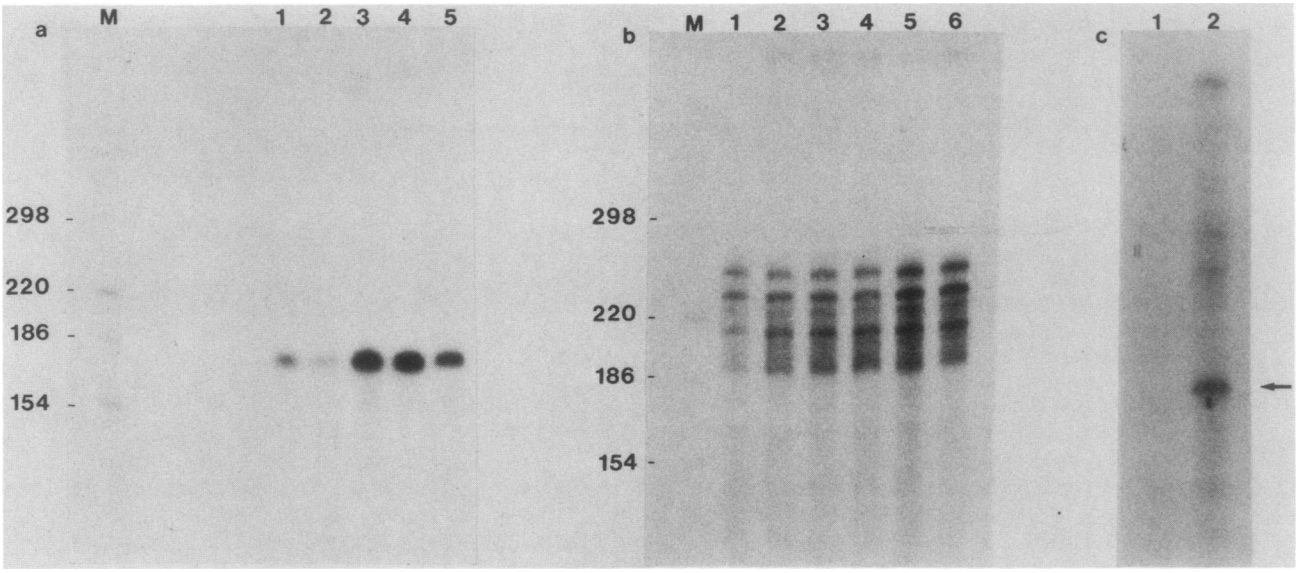

FIG. 4. Analysis of the opposite-strand RNAs. (a) The uniformly labeled *Eco*RI/*Not*I RNA probe was used to examine the levels of the opposite-strand RNAs in an equal number of 3T6 R50 cells from 2, 6, 8, and 10 h (lanes 1 through 4 respectively) and in an equivalent amount of 3T6 R50 total RNA from asynchronous cells (lane 5). (b) The uniformly labeled *Eco*RI/*Hin*dIII RNA probe was used to examine the 5′ ends of the opposite-strand RNAs in 2-, 6-, 8-, 10-, 12-, and 16-h 3T6 R50 RNA (lanes 1 through 6, respectively). (c)The levels of the opposite-strand RNAs in the 200–1 cell line were determined using cytoplasmic (lane 1) and nuclear (lane 2) RNA with *Eco*RI/*Not*I RNA probe. The arrow indicates the band representing the opposite-strand RNAs.

polyadenylation sites throughout the cell cycle. Kaufman and Sharp (13) suggest that alternative utilization of polyadenylation signals occurs during the growth regulation of a modular gene containing the major late promoter of adenovirus 2 (including the first 5′ splice site), a 3′ splice site from an immunoglobulin gene, mouse DHFR cDNA, pBR322 vector sequences, and a simian virus 40 polyadenylation signal. We feel that their conclusions about the growth regulation of these constructs are not comparable to our studies on the cell-cycle regulation of the normal DHFR gene.

The purpose of the multiple polyadenylation sites of the DHFR gene is still unclear. Of the four major DHFR mRNAs, only the 1,600-nucleotide mRNA has the hexanucleotide AAUAAA near the 3′ end. Although the variation, UAUAAG, is found 27 nucleotide upstream of the 750-nucleotide mRNA 3′ end, the other 3′ ends do not contain this sequence or any other previously identified natural variation (1). The two minor bands between the 750- and 1,000-nucleotide mRNA 3′ ends would map to +686 and +764 if they are colinear with the DHFR coding sequences. These also would not utilize any of the accepted polyadenylation signals. There are so many short stretches of A's and T's in the DHFR 3′ noncoding region that it is difficult to determine which specific sequences function as polyadenylation signals. However, sequences 3′ to the 1,600-nucleotide mRNA can influence the choice of polyadenylation sites. This is evident in the cell line 3C4 500 (Gasser and Schimke, submitted). This cell line was constructed by transfecting a DHFR minigene, containing 3′ sequences extending to the 1,600-nucleotide mRNA polyadenylation site, into DHFR-dificient hamster cells. As described by Gasser and Schimke (submitted), the majority of RNAs produced from this DHFR gene have endpoints beyond the 1,600-nucleotide mRNA in the hamster sequences. When RNA from this cell line was used in RNA experiments, it was found that although all of the normal polyadenylation sites were used, the ratios had changed (data not shown). The 1,000-nucleotide polyadenylation site was greatly enhanced, as was the larger of the two minor bands described above. Also, a faint ladder of bands could be visualized between the 800- and 1,000-nucleotide mRNA bands, indicating that the specificity of polyadenylation was reduced in this cell line. Since this cell line produces one DHFR protein of correct size, it is clear that the length of the 3′ noncoding region does not influence the translation of the gene.

Although the function of the opposite-strand transcripts from the DHFR promoter is still unknown, all evidence suggests that they are not responsible for cell-cycle regulation of the DHFR gene. It has been shown previously (Gasser and Schimke, submitted) that a transfected DHFR minigene that contains less than 340 base pairs of 5′-flanking sequence still cell-cycle regulates. This deletion removes all but approximately 50 nucleotides of the sequences coding for the opposite-strand RNAs, conserving only the 5′ ends. In addition, we have shown here that a cell line, 200–1, that has lost the ability to cell-cycle regulate still produces the opposite-strand RNAs.

Several lines of evidence indicate that cell-cycle regulation is modulated at the promoter region. First, a brief six- to sevenfold increase in transcription rate occurs at the G1/S boundary (9). Second, transfected DHFR minigenes that are truncated 200 to 300 nucleotides upstream of the start site can regulate, but those containing 50 to 100 bases less of the 5′ sequences cannot (Gasser and Schimke, submitted). Finally, the fact that both DHFR mRNAs and the opposite-strand RNAs increase at the same point in the cell cycle implies that the mechanism responsible for regulation is manifested simply by transiently increasing the efficiency of transcription at the DHFR promoter. The timing of this increase correlates with the shift into S phase, not with the number of hours after mitotic selection. Different populations of cells have G1 periods that extend for slightly different times, as monitored by [^{3}H]thymidine incorpora-

tion. Because of this, the timing of the transcription rate increase and subsequent RNA accumulation can vary from experiment to experiment. For example, in the mitotic selection in Fig. 2a, lanes 1 through 4, the increase did not occur until after 6 h, whereas in a separate mitotic selection (lanes 5 through 8) the increase had already occurred at 6 h. Also, as cell populations age, the tightness of their synchrony decays, resulting in a broader window for the transcription rate increase and giving the appearance of a less striking increase at the G1/S boundary. The best results, therefore, are obtained by using newly thawed cells for the mitotic selections and monitoring their cell cycle by [^{3}H]thymidine incorporation throughout the experiment (see reference 9 for details).

The cell-cycle regulation of the DHFR gene may be linked with replication. Mariani and Schimke (15) have shown that in hamster cells the DHFR gene is among the first sequences replicated as the cells make the transition from G1 to S phase. Correspondingly, Farnham and Schimke (9) have shown that the transient burst of transcription of the DHFR gene is also at the G1/S boundary in mouse 3T6 cells. Current experiments in this laboratory involve measuring both of these parameters in a single experiment so that a more precise view of the interactions of replication and cell-cycle regulation can be obtained.

It is also possible that cell-cycle regulation of DHFR is modulated by a transcription factor(s) whose synthesis or degradation is cell-cycle regulated. Although Dynan et al. (W. S. Dynan, S. Sazer, R. Tjian, and R. Schimke, submitted for publication) have shown that the factor SP1 can stimulate transcription from the DHFR promoter, the levels of SP1 throughout the cell cycle have not been examined. Perhaps the level of SP1 is constant throughout the cell cycle but, in combination with the increased abundance in S phase of a general cell-cycle-regulated factor such as E1a (2), is responsible for the transcription rate increase of the DHFR gene.

ACKNOWLEDGMENTS

We thank John Feder for the generous gift of 200–1 RNA and Shelley Sazer for allowing us to refer to unpublished data.

This research was funded by a Public Health Service grant from the National Institutes of Health to R.T.S. (CA 16318). P.J.F. is a recipient of a National Institutes of Health Postdoctoral Fellowship.

LITERATURE CITED

1. **Birnstiel, M. L., M. Busslinger, and K. Strub.** 1985. Transcription termination and 3′ processing: the end is in site. Cell **41**:349–359.
2. **Brown, P. C., S. M. Beverly, and R. T. Schimke.** 1981. Relationship of amplified dihydrofolate reductase genes to double minute chromosomes in unstably resistant mouse fibroblast cell lines. Mol. Cell. Biol. **1**:1077–1083.
3. **Crouse, G. F., A. Frischauf, and H. Lehrach.** 1983. An integrated and simplified approach to cloning into plasmids and single-stranded phages. Methods Enzymol. **101**:78–89.
4. **Crouse, G. F., E. J. Leys, R. N. McEwan, E. G. Frayne, and R. E. Kellems.** 1985. Analysis of the mouse *dhfr* promoter region: existence of a divergently transcribed gene. Mol. Cell. Biol. **5**:1847–1858.
5. **Crouse, G. F., C. C. Simonsen, R. N. McEwan, and R. T. Schimke.** 1982. Structure of amplified normal and variant dihydrofolate reductase genes in mouse sarcoma S180 cells. J. Biol. Chem. **257**:7887–7897.
6. **Dagert, M. and S. D. Ehrlich.** 1979. Prolonged incubation in calcium chloride improves the competence of *E. coli* cells. Gene **6**:23–28.
7. **Davis, R. W., D. Botstein, and J. R. Roth.** 1980. Advanced bacterial genetics. Cold Spring Harbor Laboratory, Cold Spring Harbor, N.Y.
8. **Farnham, P. J., J. M. Abrams, and R. T. Schimke.** 1985. Opposite-strand RNAs from the 5′ flanking region of the mouse dihydrofolate reductase gene. Proc. Natl. Acad. Sci. USA **82**:3978–3982.
9. **Farnham, P. J., and R. T. Schimke.** 1985. Transcription regulation of mouse dihydrofolate reductase in the cell cycle. J. Biol. Chem. **260**:7675–7680.
10. **Gasser, C. S., C. C. Simonsen, J. W. Schilling, and R. T. Schimke.** 1982. Expression of abbreviated mouse dihydrofolate reductase genes in cultured hamster cells. Proc. Natl. Acad. Sci. USA **79**:6522–6526.
11. **Hann, S. R., C. B. Thompson, and R. N. Eisenman.** 1985. c-myc oncogene protein synthesis is independent of the cell cycle in human and avian cells. Nature (London) **314**:366–369.
12. **Kao, H.-T., O. Capasso, N. Heintz, and J. R. Nevins.** 1985. Cell cycle control of the human HSP70 gene: implications for the role of a cellular E1a-like function. Mol. Cell. Biol. **5**:628–633.
13. **Kaufman, R. J., and P. A. Sharp.** 1983. Growth-dependent expression of dihydrofolate reductase mRNA from modular cDNA genes. Mol. Cell. Biol. **3**:1598–1608.
14. **Maniatis, T., E. F. Fritsch, and J. Sambrook.** 1982. Molecular cloning. Cold Spring Harbor Laboratory, Cold Spring Harbor, N.Y.
15. **Mariani, B. D., and R. T. Schimke.** 1984. Gene amplification in a single cell cycle in chinese hamster ovary cells. J. Biol. Chem. **259**:1901–1910.
16. **McGrogan, M., C. C. Simonsen, D. T. Smouse, P. J. Farnham, and R. T. Schimke.** 1985. Heterogeneity at the 5′ termini of mouse dihydrofolate reductase mRNAs. J. Biol. Chem. **260**: 2307–2314.
17. **Setzer, D. R., M. McGrogan, J. H. Nunberg, and R. T. Schimke.** 1980. Size heterogeneity in the 3′ end of dihydrofolate reductase messenger RNAs in mouse cells. **22**:361–370.
18. **Setzer, D. R., M. McGrogan, and R. T. Schimke.** 1982. Nucleotide sequence surrounding multiple polyadenylation sites in the mouse dihydrofolate reductase gene. J. Biol. Chem. **257**: 5143–5147.
19. **Thompson, C. B., P. B. Challoner, P. E. Neiman, and M. Groudine.** 1985. Levels of c-myc oncogene mRNA are invarient throughout the cell cycle. Nature (London) **314**:363–366.